

Received November 26, 2020, accepted December 7, 2020, date of publication December 9, 2020,
date of current version December 21, 2020.

Digital Object Identifier 10.1109/ACCESS.2020.3043721

A High-Precision Motion Control Based on a Multi-Rate Periodic Adaptive Disturbance Observer of a Linear Actuator for High Load Systems

KWANGHYUN CHO¹, (Member, IEEE), AND KANGHYUN NAM², (Member, IEEE)

¹Manufacturing Technology Center, Samsung Electronics Company Ltd., Gyeonggi-do 443-742, South Korea

²School of Mechanical Engineering, Yeungnam University, Gyeongsan 712-749, South Korea

Corresponding author: Kanghyun Nam (khn timer@yu.ac.kr)

This work was supported by the Korea Institute for Advancement of Technology (KIAT) grant funded by the Korea Government (MOTIE) (HRD Program for Industrial Innovation) under Grant P0008473.

ABSTRACT This study is concerned with the problem of compensating for periodic disturbances under repetitive motion conditions. In order to achieve high precision positioning for high load systems with periodic disturbances, a practical motion control scheme based on a multi-rate periodic adaptive disturbance observer (MPADOB) is proposed. Nonlinear disturbances such as the force ripple, friction force, and cable tension force occur when linear actuators for high load systems are used on linear motors with iron-cores. These disturbances are obstacles to achieving high-precision control. In the proposed scheme, these disturbances are attenuated perfectly by using a periodic feedback loop. However, the memory size becomes large when the repetitive motions increase since the periodic feedback loop has many sample delay terms. It is a weakness in the control schemes that use a periodic feedback loop, although it can improve the control performance. In this study, the multi-rate periodic feedback loop and a predictive estimator have been proposed to improve the memory size issues for practical implementation and control performance. Using MPADOB, the control schemes that use periodic feedback loop can be applied to a variety of industrial applications practically. The effectiveness of the proposed scheme is verified by a variety of experimental tests.

INDEX TERMS High-precision motion control, disturbance observer, periodic disturbance, linear actuator, high load system.

I. INTRODUCTION

High load systems have been used in various assembly lines such as LCD/OLED panel transportation systems, semi-conductor fabrication equipment, and inspection machines. In the past, these systems have required only high-speed/high-acceleration motions due to separated unit processes such as transportation, assembly, and fabrication process [1]–[4]. Based on previous studies, these separated processes can occur simultaneously. A high-precision motion is also required to satisfy the increasing demands on higher productivity as saving process time. Therefore, linear actuators based on linear motors are utilized widely for

high load systems due to their high force densities and high efficiencies.

However, these linear actuators have some challenges in achieving high-precision position control and high speed/acceleration control simultaneously [5], [6]. Since the linear actuators based on linear motors contain the mover's iron-cores, it is directly affected by the force ripple, including the detent force that occurs due to the attraction between the iron-cores of the mover and the permanent magnets or irregular magnetic field of the permanent magnets. The force ripple has a fundamental period similar to the pole pitch of permanent magnets. Since its frequency becomes higher as increasing the mover's moving speed, it is challenging to attenuate the effect of the force ripple by general feedback control schemes, especially in high load systems

The associate editor coordinating the review of this manuscript and approving it for publication was Jun Shen¹.

requiring fast-moving speed. The friction force is also another obstacle to achieving high-precision control. In the case of high load motion systems using ball bearing guides, motion accuracy and resolution may be limited due to guide friction [7]. The friction force has heavy nonlinear characteristics at low-velocity motions depending on the position and the velocity.

Numerous control methods to achieve high-precision position control and high speed/acceleration control have already been proposed. The control scheme based on a compact model of the force generation that includes the effect of the ripple disturbance has been proposed in [8] and [9]. A variety of friction force models such as the generalized Maxwell-slip (GMS) model, variable natural length spring (VNLS) model, and rheology-based model have been used to attenuate the effect of friction force [10]–[12]. The disturbance observer-based control schemes are also good to compensate for non-linear disturbances [13], [14]. Since these models contain various parameters to be identified, it is difficult to guarantee that all the estimated parameters will converge to their actual values.

However, the control schemes using periodic feedback loops such as learning control (PALC), repetitive control (RC), and iterative learning control (ILC) are very powerful to compensate for these disturbances. Since the periodic feedback loops guarantee the characteristics of non-causality about the estimated disturbances, it is very effective to attenuate these periodic disturbances without mathematical models. In [15], PALC was proposed to compensate for these periodic disturbances effectively. In [16] and [17], RC was presented to eliminate the periodic tracking error and unmodeled disturbances. In [18] and [19], ILC was presented to enhance conventional PID feedback control performance. The authors also proposed a periodic adaptive disturbance observer (PADOB) to compensate for the disturbance [20]. However, in these schemes, we make the memory size big because the periodic feedback loop has many sample delay terms when the period of repetitive motion is increased. Even though these schemes can improve control performance, it is a fatal weakness of these schemes using the periodic feedback loop.

This study is concerned with the problem of compensating for periodic disturbances under repetitive motion conditions. In this study, a novel high-precision motion control method is proposed to achieve high-precision position control and high speed/acceleration control in high load systems. We called the method a multi-rate periodic adaptive disturbance observer (MPADOB). The proposed scheme utilizes a periodic feedback loop to compensate for a lumped disturbance perfectly. To improve the memory size issue about the periodic feedback loop, a multi-rate periodic feedback loop has been proposed. The predictive estimator is used to compensate for down-sampled periodic feedback loop. By using MPADOB, the control schemes with the periodic feedback loop such as ILC, RC, PALC and PADOB can be applied to various industrial applications practically.

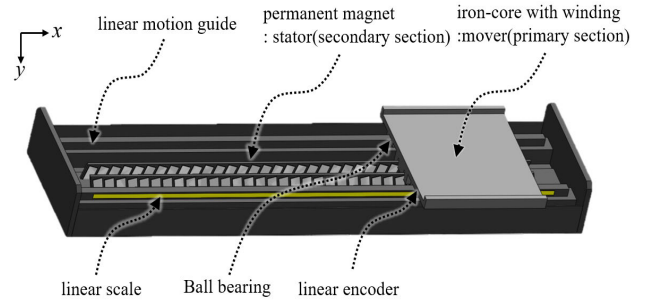


FIGURE 1. Linear actuator for a high load system.

The rest of this paper is organized as follows. In section II, a linear actuator for high load systems and its mathematical model are introduced. In section III, a multi-rate periodic adaptive disturbance (MPADOB) is presented, while the experimental tests in various conditions are carried out to verify the performance of the proposed MPADOB in section IV. In section V, a summary of the paper is presented to conclude it.

II. PROBLEM FORMULATION

In this section, a linear actuator for high load systems and its mathematical model are illustrated.

A. HIGH LOAD LINEAR ACTUATOR

In general, linear actuators for high load systems are based on linear motors which are made up of the primary section (armature) and secondary section (field magnet). According to the interaction between the primary section and secondary section and those physical characteristics, there are many types of linear actuators [22].

The physical structure of the linear actuator used in this study is shown in Fig. 1. The primary section is wound by coils with iron-core, while the secondary section is made up of many permanent magnets. It has high force density/high efficiency and can achieve high-acceleration motion due to the iron-core of the primary section. However, it also has many difficulties in achieving high accuracy positioning because of the force ripple and friction force.

The force ripple occurs by the detent force generated by the mutual attraction between the magnets and iron-core of the mover when the applied force is zero. The irregular magnetic field of the permanent magnets and inaccuracy in electronic commutation by the servo amplifier also make the force ripple. It causes a periodic variation of the force constant. The force ripple depends on the relative position of the mover with respect to the magnets [8]. Assuming that the pole pitch of the magnets is x_p , and the velocity of the mover is \dot{x} , the frequency of the force ripple induced by the detent force is given by $\Omega_{det} = 2\pi/x_p\dot{x}$. The force ripple induced by the reluctance force has a fundamental frequency of $\Omega_{rel} = 6\pi/x_p\dot{x}$. The constant offset of current sensors also makes the force ripple with a frequency of $\Omega_{rel} = \pi/x_p\dot{x}$. Therefore,

the force ripple has a variety of frequency components, and its fundamental frequency is varied by the velocity of the mover \dot{x} . The friction force is induced due to ball bearing and linear motion guides. The linear motion guide with ball bearing can support a high load, but motion accuracy and resolution may be limited due to guide friction. Therefore, the force ripple and friction force should be compensated to achieve high precision positioning in high load systems using linear actuators.

B. MATHEMATICAL MODEL

The mathematical model of the linear actuator for high load systems is presented as follows:

$$M\ddot{x}(t) = -B\dot{x}(t) + u(t) - F_{fric}(x, \dot{x}) - F_{rip}(x) - F_{load}(t) \quad (1)$$

where $x(t)$, $\dot{x}(t)$, and $\ddot{x}(t)$ are position, velocity and acceleration of the mover, respectively, M the mass of the mover, B the viscous friction coefficient, $u(t)$ control input, $F_{fric}(x, \dot{x})$ the friction force, $F_{rip}(x)$ the force ripple including the detent force, and reluctance force, and $F_{load}(t)$ the load disturbance. For simplicity, the load disturbances and electrical dynamics are ignored because the load disturbance is a nearly constant and the electrical dynamics is fast enough comparing with the frequency bandwidth of the interest [23].

Assuming that the mass and viscous friction coefficient are known by a system identification procedure, a nominal model is obtained from (1) as follows:

$$M_n\ddot{x}(t) = -B_n\dot{x}(t) + u(t) + d(t), \quad (2)$$

where M_n and B_n are the known nominal values of the mass and viscous friction coefficient, respectively.

In (2), $d(t)$ is a lumped disturbance, which includes the friction force, the force ripple, and the parametric errors multiplied by acceleration and velocity. It can be written as follows:

$$d(t) = -\Delta M\ddot{x}(t) - \Delta B\dot{x}(t) - F_{fric}(x, \dot{x}) - F_{rip}(x), \quad (3)$$

where $\Delta M = M - M_n$ and $\Delta B = B - B_n$ mean the parametric errors of the mass and viscous friction coefficient, respectively.

The control objective is to track the desired position $x_d(t)$ and the corresponding desired velocity $\dot{x}_d(t)$ given for a linear actuator in high load system. The tracking errors should be minimized as much as possible.

III. MULTI-RATE PERIODIC ADAPTIVE DISTURBANCE OBSERVER

In this section, the proposed control scheme which is MPADOB is illustrated in detail. The memory size issue of a periodic adaptive disturbance observer (PADOB) is improved by the proposed scheme, MPADOB [20].

A. ASSUMPTIONS AND PROPERTIES

The tasks required by the linear actuator for high load systems have the following assumptions.

- *Assumption 1:* The given task for the high load motion system is to track periodic position trajectories under the same operating conditions repetitively.
- *Assumption 2:* The induced disturbances in the high load motion system are state-dependent such as position, velocity and acceleration of the mover as shown in (3). These disturbances are identical for each repetitive time period due to repetitive motion conditions.

From these assumptions, all the measured states and disturbances have the following properties.

Property 1 (Periodicity of the Desired and Measured States):

From *Assumption 1*, when the desired trajectories with the repetitive time period T_r are given as:

$$x_d(t) = x_d(t - T_r), \dot{x}_d(t) = \dot{x}_d(t - T_r), \ddot{x}_d(t) = \ddot{x}_d(t - T_r),$$

it can be considered that the measured states are also periodic and they have the same time period T_r if a tracking error between the desired and measured states is minimized.

$$x(t) \approx x(t - T_r), \dot{x}(t) \approx \dot{x}(t - T_r), \ddot{x}(t) \approx \ddot{x}(t - T_r).$$

Property 2 (Periodicity of Disturbance):

From *Assumption 2*, the induced disturbance has the repetitive time period T_r given as:

$$d(t) \approx d(t - T_r).$$

B. CONTROLLER DESIGN

The structure of the controller is described in Fig. 2. All control inputs are designed by the nominal model (2) as follows:

$$u(t) = u_{ff}(t) + u_{fb}(t) - \hat{d}(t), \quad (4)$$

$$u_{ff}(t) = M_n\ddot{x}_d(t) + B_n\dot{x}_d(t), \quad (5)$$

$$u_{fb}(t) = K_{fb} \cdot \sigma(t) + M_n(\alpha\dot{e}_x(t) + \beta e_x(t)) - B_n\dot{e}_x(t), \quad (6)$$

where

$$\sigma(t) = \dot{e}_x(t) + \alpha e_x(t) + \beta \int_0^t e_x(r)dr. \quad (7)$$

Here, $u_{ff}(t)$ is the feedforward control input based on the known parameters, $u_{fb}(t)$ is the feedback control input, and $\hat{d}(t)$ is the periodic adaptation law that means the estimated disturbance. K_{fb} , α and β are positive tuning parameters. In (6) and (7), $e_x(t)$ means error between the desired and measured position, i.e., $e_x(t) = x_d(t) - x(t)$. $\dot{e}_x(t)$ induces the derivative of $e_x(t)$.

The periodic adaptation law of the lumped disturbance is designed as follows:

$$\hat{d}(t) = \hat{d}_f(t - T_r) - K_a\sigma(t), \quad (8)$$

where K_a is an adaptation gain that determines the adaptation speed which should be positive number. $\hat{d}_f(t - T_r)$ means the periodic feedback loop.

$$\hat{d}_f(t - T_r) = H[\hat{d}(t - T_r)] = \sum_{k=-n}^n c_{|k|} z^{-k} \hat{d}(t - T_r). \quad (9)$$

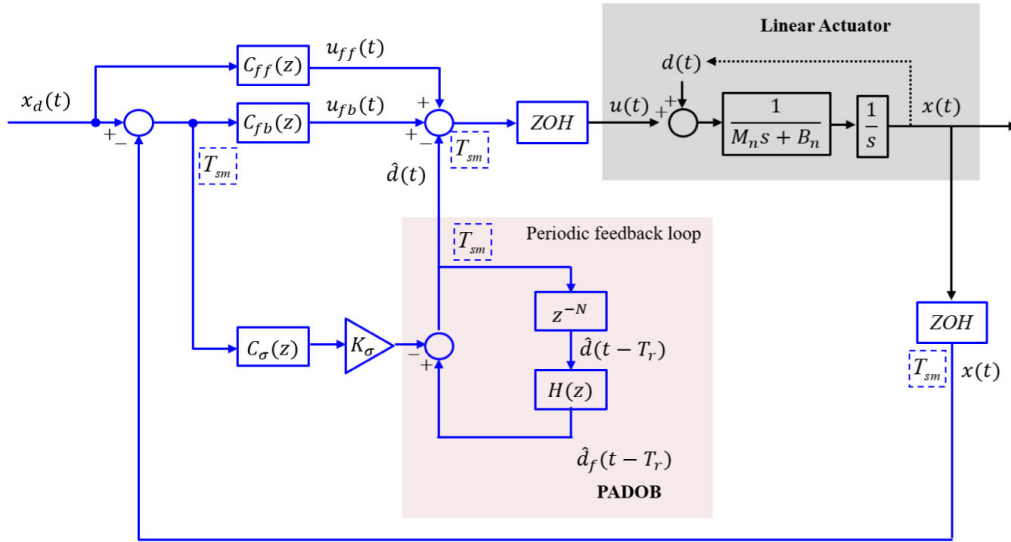


FIGURE 2. Block diagram of the PADOB.

$H[\cdot]$ is a zero-phase low pass filter (ZPF) with n -th order of the filter, and z^{-k} a k -step time delay. $c_{|k|}$ is the normalized coefficient of the filter, which has a property as $2 \sum_{k=1}^n c_k + c_0 = 1$. The ZPF is utilized to guarantee the stability of the overall system from unmodeled dynamics or uncertainties. In the frequency range to be compensated for disturbances, $\hat{d}_f(t - T_r)$ is equal to $\hat{d}(t - T_r)$ since there are no phase delay and magnitude attenuation due to non-causal characteristic of the periodic feedback loop. To prove the stability of the closed-loop system with the designed controllers and adaptation law, (8) is rewritten as follows:

$$\begin{aligned} \hat{d}(t) &= \hat{d}_f(t - P_t) - K_a \sigma(t) \\ &= \hat{d}(t - P_t) - \hat{d}_h(t - P_t) - K_a \sigma(t). \end{aligned} \quad (10)$$

Here, $\hat{d}_h(t - P_t)$ is the high frequency component of the estimated disturbance at the previous time period that is eliminated by ZPF.

Consider the following positive Lyapunov candidate function:

$$V(t) = \frac{1}{2} \sigma^2(t) + \frac{1}{2K_a M_n} \int_{t-P_t}^t \tilde{d}^2(r) dr, \quad (11)$$

where $\tilde{d}(t) = d(t) - \hat{d}(t)$.

Since it can be considered that the periodic disturbance approximated in *Property 2* consists of the dominant periodic and partial non-periodic components due to based on our *Assumptions* and *Properties*, the actual disturbance $d(t)$ can be represented as follow:

$$d(t) = d(t - T_r) + d_n(t), \quad (12)$$

where $d_n(t)$ is the non-periodic disturbance. The disturbances such as unmodeled dynamics, the high frequency noise, and the switching friction force induced by the difference in speed reversal moments at each time period can be considered as $d_n(t)$.

Then, the difference between the positive Lyapunov candidate functions at two discrete time points (t and $t - T_r$) is calculated as follows:

$$\begin{aligned} \Delta V(t) &= V(t) - V(t - T_r) \\ &= \frac{1}{2} \sigma^2(t) - \frac{1}{2} \sigma^2(t - T_r) \\ &\quad + \frac{1}{2K_a M_n} \int_{t-T_r}^t [\tilde{d}^2(r) - \tilde{d}^2(r - T_r)] dr. \end{aligned} \quad (13)$$

For simplicity of the calculation, we assume that the first two terms at the right hand side of (13) be denoted by $\Delta V_1(t)$ and the integral term by $\Delta V_2(t)$. Then, $\Delta V_1(t)$ is calculated as follows:

$$\begin{aligned} \Delta V_1(t) &= \frac{1}{2} \sigma^2(t) - \frac{1}{2} \sigma^2(t - T_r) = \int_{t-T_r}^t \sigma_1(r) \dot{\sigma}_1(r) dr \\ &= -\frac{1}{M_n} \int_{t-T_r}^t [K_{fb} \sigma^2(r) + \tilde{d}(r) \sigma(r)] dr \end{aligned} \quad (14)$$

$\Delta V_2(t)$ is also calculated as follows:

$$\begin{aligned} \Delta V_2(t) &= \frac{1}{2K_a M_n} \int_{t-T_r}^t [\tilde{d}^2(r) - \tilde{d}^2(r - P_t)] dr \\ &= \frac{1}{M_n} \int_{t-T_r}^t \tilde{d}(r) \sigma(r) dr \\ &\quad + \frac{1}{2K_a M_n} \int_{t-T_r}^t [2d_n(r) \tilde{d}(r) - (d_n(r) + K_a \sigma(r))^2] dr \end{aligned} \quad (15)$$

When the non-periodic disturbance and the estimation error of the lumped disturbance are bounded as given:

$$|d_n(t)| < \sqrt{\eta_1}, \quad \text{where } \eta_1 \geq 0, \quad (16)$$

$$|\tilde{d}(t)| < \sqrt{\eta_2}, \quad \text{where } \eta_2 \geq 0, \quad (17)$$

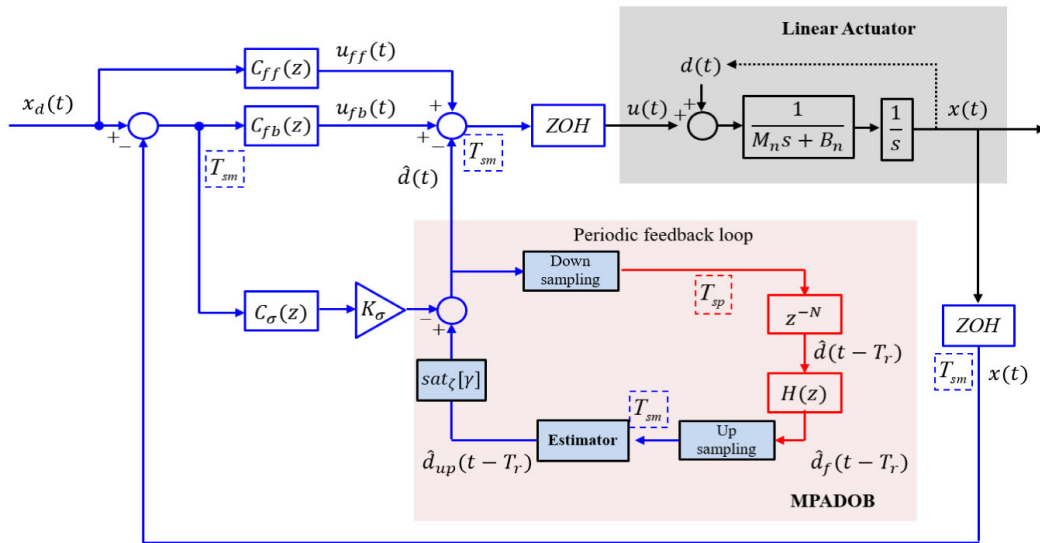


FIGURE 3. Block diagram of the MPADOB.

then, (15) can be recalculated using Cauchy-Schwarz inequality as follows:

$$\Delta V_2(t) \leq \frac{1}{M_n} \int_{t-T_r}^t \tilde{d}(r)\sigma(r)dr + \frac{1}{2K_a M_n} \int_{t-T_r}^t \eta dr, \quad (18)$$

Here, η induces $\eta = \eta_1 + \eta_2$. And then, the difference in ΔV becomes:

$$\begin{aligned} \Delta V(t) &= \Delta V_1(t) + \Delta V_2(t) \\ &\leq -\frac{1}{2K_a M_n} \int_{t-T_r}^t (2K_{fb}K_a\sigma^2(r) - \eta)dr. \end{aligned} \quad (19)$$

The difference $\Delta V(t)$ becomes negative semi-definite when the following condition is guaranteed

$$2K_{fb}K_a\sigma^2(r) \geq \eta, \quad (20)$$

Here, (20) can be guaranteed by large K_{fb} and K_a or the tracking errors with certain boundary level for any K_{fb} and K_a . Therefore, it can be proved theoretically that the system is stable if there exist a non-periodic disturbance. The control parameters should be selected by considering the limitation of the control input and the instability problem of time response induced by the unmodeled dynamics.

C. MULTI-RATE PERIODIC ADAPTIVE DISTURBANCE OBSERVER

Since the periodic adaptation law in (8) utilizes the periodic feedback loop, the estimated disturbance at the previous iteration, $\hat{d}(t - T_r)$, should be saved in the memory as a lot of time delay terms. The number of used delay is determined by the time period of the reference trajectory T_r and the sample time of the periodic feedback loop T_{sp} . In the case where the periodic feedback loop with the same control loop time T_{sm} is executed, the number of delay terms is $N = T_r/T_{sm}$. The number of delay terms must be increased as the time period of the reference trajectory increases and the sampling time of

the controller decreases. Therefore, the memory size issue is a very important problem in a variety of industry application where this scheme is used practically.

In this study, the issues about memory size in control schemes using the periodic feedback loop can be improved by reducing the number of delay utilized for the periodic feedback loop. As shown in Fig. 3, when the sample time of the periodic feedback loop T_{sp} is identical with the sample time of total controller T_{sm} (i.e., $T_{sp} = T_{sm}$), the total position controller becomes PADOB based controller, and the number of delay utilized for the periodic feedback loop is determined as $N = T_r/T_{sm}$. When both control loop times (T_{sm} and T_{sp}) are increased simultaneously, the utilized memory size can be reduced. But, the tracking performance can be worse since the performance of the feedback controller becomes worse. To prevent the deterioration of total tracking performance, it is possible to increase only the sample time of the periodic feedback loop T_{sp} . In the case that the sample time of the periodic feedback loop is increased (i.e., $T_{sm} < T_{sp}$), the number of the utilized delay is reduced to $N = T_r/T_{sp}$. This controller is called the multi-rate PADOB (MPADOB) because two different sample times (i.e., $T_{sp} \neq T_{sm}$) are utilized in PADOB.

In MPADOB, the tracking performance can be different depending on how the down-sampled periodic feedback $\hat{d}_f(t - T_r)$ is compensated when it is up-sampled to $\hat{d}_{up}(t - T_r)$ in Fig.2. As shown in Fig.4, we proposed two MPADOB schemes in this study:

- H-MPADOB(Hold method)

The periodic feedback is held (H-MPADOB) when it is up-sampled with no compensation.

$$\begin{aligned} t = 0 : \hat{d}_{up}(0 - T_r) &= \hat{d}_f(0 - T_r) \\ t = T_{sm} : \hat{d}_{up}(T_{sm} - T_r) &= \hat{d}_f(0 - T_r) \end{aligned}$$

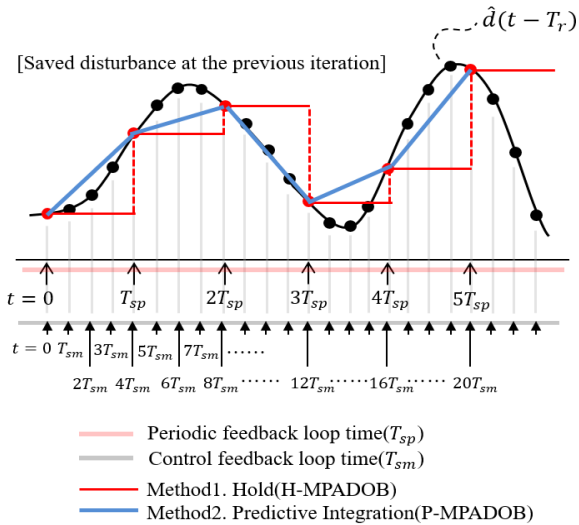


FIGURE 4. Hold / Predictive Integration Multi-rate PADOB.

$$\begin{aligned}
 t = 2T_{sm} : \hat{d}_{up}(2T_{sm} - T_r) &= \hat{d}_f(0 - T_r) \\
 &\vdots \\
 t = kT_{sm} : \hat{d}_{up}(kT_{sm} - T_r) &= \hat{d}_f(T_{sp} - T_r) \\
 t = (k + 1)T_{sm} : \\
 \hat{d}_{up}((k + 1)T_{sm} - T_r) &= \hat{d}_f(T_{sp} - T_r) \\
 &\vdots
 \end{aligned} \tag{21}$$

• P-MPADOB(Predictive integration method)

The predictive integration method (P-MPADOB) is used to estimate the disturbance when there is no samples in the periodic feedback loop. Owing to the fact that the slope of the down-sampled periodic feedback can be known in advanced, the periodic feedback at the current sample time in the previous iteration can be predicted, and the hold action can also be compensated.

$$\begin{aligned}
 t = 0 : \hat{d}_{up}(0 - T_r) &= \hat{d}_f(0 - T_r) \\
 t = T_{sm} : \hat{d}_{up}(T_{sm} - T_r) \\
 &= \hat{d}_f(0 - T_r) + T_{sm} \frac{\hat{d}_f(T_{sp} - T_r) - \hat{d}_f(0 - T_r)}{T_{sp}} \\
 t = 2T_{sm} : \hat{d}_{up}(2T_{sm} - T_r) \\
 &= \hat{d}_{up}(T_{sm} - T_r) + T_{sm} \frac{\hat{d}_f(T_{sp} - T_r) - \hat{d}_f(0 - T_r)}{T_{sp}} \\
 &\vdots \\
 t = kT_{sm} : \hat{d}_{up}(kT_{sm} - T_r) &= \hat{d}_f(T_{sp} - T_r) \\
 t = (k + 1)T_{sm} : \hat{d}_{up}((k + 1)T_{sm} - T_r) \\
 &= \hat{d}_{up}(kT_{sm} - T_r) + T_{sm} \frac{\hat{d}_f(2T_{sp} - T_r) - \hat{d}_f(T_{sp} - T_r)}{T_{sp}} \\
 &\vdots
 \end{aligned} \tag{22}$$

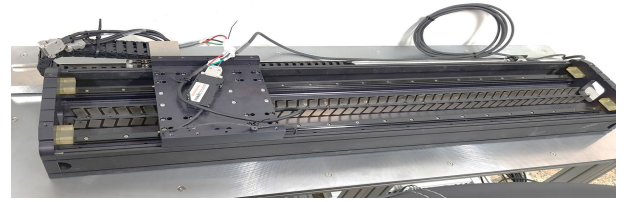


FIGURE 5. Experimental high load system.

In H-MPADOB, the hold action is very simple, but it may aggravate the tracking performance since the estimated disturbance at the previous iteration cannot describe the actual disturbance. However, P-MPADOB can improve the tracking performance of H-MPADOB since the down-sampled periodic feedback is compensated by the predictive integration method.

Using (21) and (22), the periodic adaptation law becomes as follows:

$$\hat{d}(t) = \text{sat}_\zeta [\hat{d}_{up}(t - T_r) - K_a \sigma(t)], \tag{23}$$

where

$$\text{sat}_\zeta [\gamma] = \begin{cases} -\zeta & \text{if } \gamma < -\zeta \\ \gamma & \text{if } |\gamma| \leq \zeta \\ \zeta & \text{if } \gamma > \zeta. \end{cases}$$

Here, K_a is an adaptation gain ($K_a > 0$). To prevent the divergence of the estimated lumped disturbance, we employed $\text{sat}_\zeta[\cdot]$. ζ is a design parameter which is mostly determined by the maximum value of the actual lumped disturbance.

$$\hat{d}_{up}(t - T_r) = E[\hat{d}_f(t - T_r)]. \tag{24}$$

IV. PERFORMANCE VERIFICATION

In this section, the experimental setup and results are illustrated to verify the effectiveness of the proposed control scheme.

A. EXPERIMENTAL SETUP

All experiments were carried out based on the high load system depicted in Fig. 5. PWM inverter that has 10kHz switching frequency was utilized and it was controlled by a dSPACE DS1103 board. The current and position controllers were executed at 50 μsec and 0.5 msec control loop time, respectively. An optical linear encoder with a resolution of 0.5 μm was utilized to measure the position of linear actuator.

B. EXPERIMENTAL TESTS

To verify the effectiveness of the proposed MPADOB, various comparative studies were implemented as shown in Table 1. The reference trajectories shown in Fig. 6 are used in this study, that have a time period, $T_r = 2\text{sec}$. The linear actuator for high load systems tracks these reference trajectories to minimize position tracking error.

The proposed MPADOB is done by comparing its tracking performances with other controllers as shown below:

TABLE 1. Comparative study in MPADOB.

| | T_{sm} [ms] | T_{sp} [ms] | Required delay N [sam] |
|------------|---------------|---------------|--------------------------|
| ADT04 | 0.4 | - | 1 |
| PADOB04 | 0.4 | 0.4 | 5000 |
| H-MPADOB04 | 0.4 | 4.0 | 500 |
| P-MPADOB04 | 0.4 | 4.0 | 500 |
| PADOB08 | 0.8 | 0.8 | 2500 |
| H-MPADOB08 | 0.8 | 4.0 | 500 |
| P-MPADOB08 | 0.8 | 4.0 | 500 |

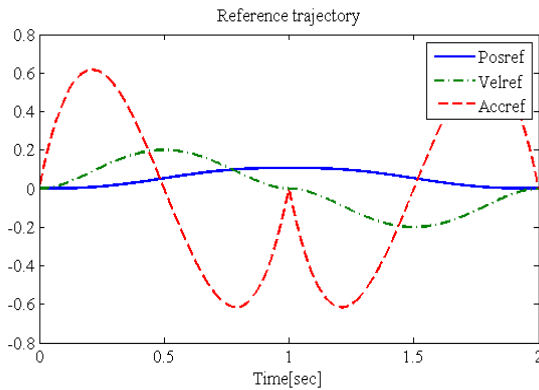


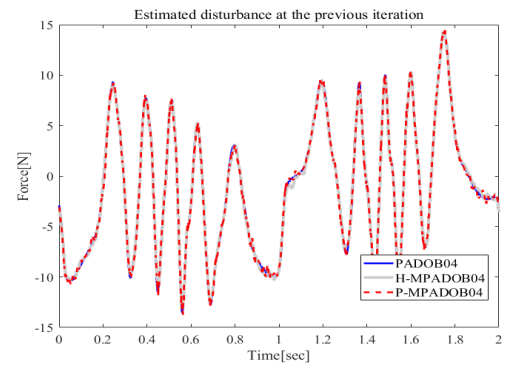
FIGURE 6. Reference trajectories.

TABLE 2. Tracking performance results for 11~20 iterations in MPADOB.

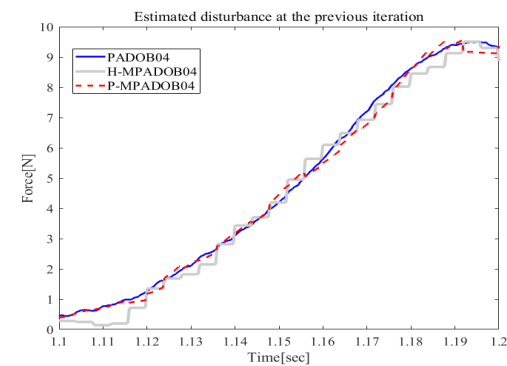
| | RMS $\ e\ _2$ [μm] | | MAX $\ e\ _\infty$ [μm] | |
|------------|---------------------------|---------|--------------------------------|---------|
| | Average | Maximum | Average | Maximum |
| ADT04 | 0.98 | 0.99 | 2.96 | 3.17 |
| PADOB04 | 0.23 | 0.25 | 0.94 | 1.13 |
| H-MPADOB04 | 0.48 | 0.50 | 1.92 | 2.18 |
| P-MPADOB04 | 0.43 | 0.44 | 1.54 | 1.74 |
| PADOB08 | 0.48 | 0.52 | 1.88 | 2.24 |
| H-MPADOB08 | 0.64 | 0.68 | 2.58 | 3.07 |
| P-MPADOB08 | 0.58 | 0.61 | 2.15 | 2.55 |

- ADT: A PID controller with adaptation laws. [21]
- PADOB: A periodic adaptive disturbance observer with the period T_{sm} of periodic feedback loop. [20]
- MPADOB: A periodic adaptive disturbance observer with the period T_{sp} of periodic feedback loop.

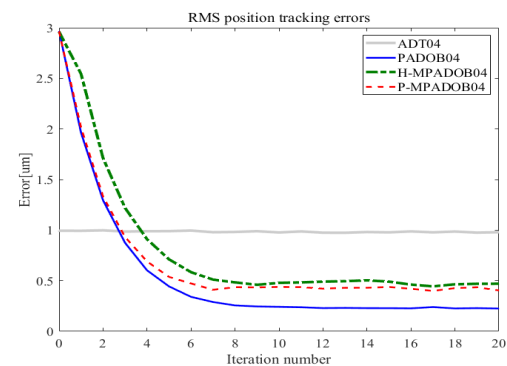
Fig. 7 shows experimental results of comparative studies. ADT utilized the sample time of 0.4 ms (noted as ‘‘ADT04’’). The experimental results when the sample time of PADOB was 0.4 ms and the sample time of the periodic feedback loop in MPADOB was 4.0 ms were presented in Fig. 7(a)~ 7(d). In this case, the numbers of utilized delay in PADOB and MPADOB were 5000 and 500. ADT showed the smallest tracking error at the 0th-iteration, but the tracking errors of PADOB and MPADOB become smaller than that of ADT as the iteration number increased. It means that the use of additional memory in the controller can improve the tracking performance. Although the number of used delays in MPADOB was reduce to 500, its tracking performance was better than that of ADT. Of course, the tracking performance of MPADOB was worse than that of PADOB due to reduced memory size. However, it was verified that the



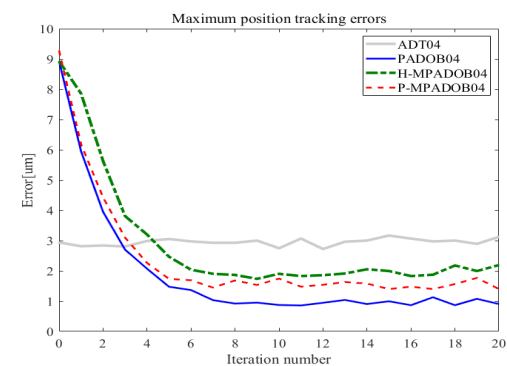
(a)



(b)



(c)



(d)

FIGURE 7. Tracking performance results in MPADOB ($T_{sm} = 0.4ms$, $T_{sp} = 4s$): (a) Estimated disturbances. (b) Enlarged estimated disturbances. (c) RMS of the tracking errors. (d) Maximum of the tracking errors.

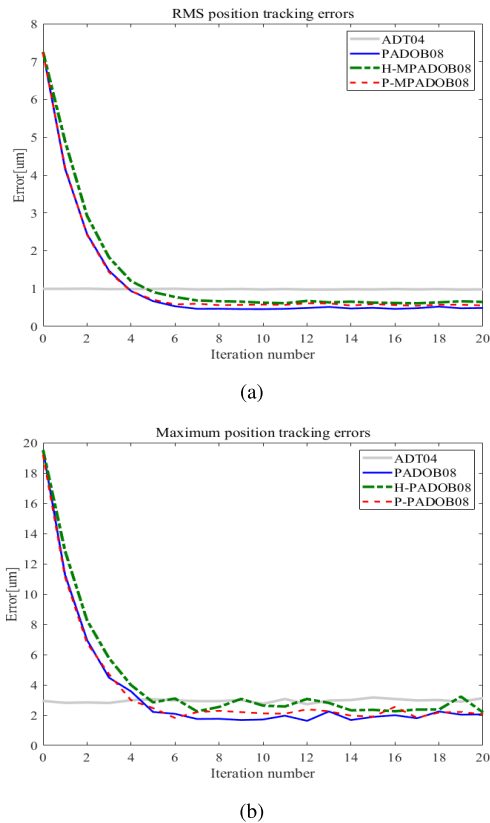


FIGURE 8. Tracking performance results in MPADOB ($T_{sm} = 0.8ms$, $T_{sp} = 4s$): (a) RMS of the tracking errors. (b) Maximum of the tracking errors.

predictive integration method (P-MPADOB04) could improve the tracking performance when it was compared with the hold method (H-MPADOB04). The estimated disturbance of P-MPADOB04 was smoother than that of H-MPADOB04 and it was similar to that of PADOB due to the predictive integration method as shown in Fig. 7(b). So the tracking errors of P-MPADOB04 reduced more than those of H-MPADOB04. Fig. 8(a) and 8(b) show the experimental results when the sample time of PADOB was 0.8 ms and the sample time of the periodic feedback loop in MPADOB was 4.0 ms. In this case, the numbers of utilized delay in PADOB and MPADOB were 2500 and 500. Although the sample time of PADOB and MPADOB were larger than that of ADT, those tracking performances were better than that of ADT. But, it was verified that increasing the sample time aggravated the tracking performances of PADOB and MPADOB, as shown in Fig. 7 and 8. From these experimental results, it is verified that the memory size issue of PADOB can be also improved by MPADOB, but the deterioration of the tracking performance cannot be avoided due to lack of samples to estimate the disturbance at the previous iteration.

V. CONCLUSION

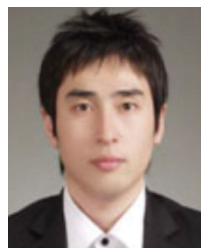
This paper presents a MPADOB using predictive estimator. To compensate for the down-sampled periodic feedback loop, a predictive estimator is designed. The performance

of MPADOB has been verified through a variety of comparative studies under repetitive motions. Our results show that a predictive estimator improves the performance of the MPADOB significantly. However, it is found that the control performance in the proposed MPADOB can be changed depending on the time period of the periodic feedback loop and its estimation results. In the future, the predictive estimator in MPADOB will be supplemented by methods to use mechanical dynamics of disturbances.

REFERENCES

- [1] M. Iwasaki, K. Seki, and Y. Maeda, "High-precision motion control techniques: A promising approach to improving motion performance," *IEEE Ind. Electron. Mag.*, vol. 6, no. 1, pp. 32–40, Mar. 2012.
- [2] K. Saiki, A. Hara, K. Sakata, and H. Fujimoto, "A study on high-speed and high-precision tracking control of large-scale stage using perfect tracking control method based on multirate feedforward control," *IEEE Trans. Ind. Electron.*, vol. 57, no. 4, pp. 1393–1400, Apr. 2010.
- [3] T. Yamaguchi, M. Hirata, and J. Pang, *High-Speed Precision Motion Control*. Boca Raton, FL, USA: CRC Press, 2011.
- [4] A. Amthor, S. Zschaek, and C. Ament, "High precision position control using an adaptive friction compensation approach," *IEEE Trans. Autom. Control*, vol. 55, no. 1, pp. 274–278, Jan. 2010.
- [5] L. Lu, Z. Chen, B. Yao, and Q. Wang, "Desired compensation adaptive robust control of a Linear-Motor-Driven precision industrial gantry with improved cogging force compensation," *IEEE/ASME Trans. Mechatronics*, vol. 13, no. 6, pp. 617–624, Dec. 2008.
- [6] R. Cao and K.-S. Low, "A repetitive model predictive control approach for precision tracking of a linear motion system," *IEEE Trans. Ind. Electron.*, vol. 56, no. 6, pp. 1955–1962, Jun. 2009.
- [7] J.-S. Chen, K.-C. Chen, Z.-C. Lai, and Y.-K. Huang, "Friction characterization and compensation of a linear-motor rolling-guide stage," *Int. J. Mach. Tools Manuf.*, vol. 43, no. 9, pp. 905–915, Jul. 2003.
- [8] L. Bascetta, P. Rocco, and G. Magnani, "Force ripple compensation in linear motors based on closed-loop position-dependent identification," *IEEE/ASME Trans. Mechatronics*, vol. 15, no. 3, pp. 349–359, Jun. 2010.
- [9] G. Ferretti, G. Magnani, and P. Rocco, "Modeling, identification, and compensation of pulsating torque in permanent magnet AC motors," *IEEE Trans. Ind. Electron.*, vol. 45, no. 6, pp. 912–920, Dec. 1998.
- [10] Z. Jamaludin, H. Van Brussel, and J. Swevers, "Quadrant glitch compensation using friction model-based feedforward and an inverse-model-based disturbance observer," in *Proc. 10th IEEE Int. Workshop Adv. Motion Control*, Mar. 2008, pp. 212–217.
- [11] H. Asaumi and H. Fujimoto, "Proposal on nonlinear friction compensation based on variable natural length spring model," in *Proc. SICE Annu. Conf.*, Aug. 2008, pp. 2393–2398.
- [12] Y. Maeda and M. Iwasaki, "Analytical examinations and compensation based on rolling friction model for slow settling response in precise positioning," *IEEJ Trans. Ind. Appl.*, vol. 129, no. 12, pp. 1218–1225, 2009.
- [13] H. Pan, W. Sun, H. Gao, and X. Jing, "Disturbance observer-based adaptive tracking control with actuator saturation and its application," *IEEE Trans. Autom. Sci. Eng.*, vol. 13, no. 2, pp. 868–875, Apr. 2016.
- [14] H. Pan and W. Sun, "Nonlinear output feedback finite-time control for vehicle active suspension systems," *IEEE Trans. Ind. Informat.*, vol. 15, no. 4, pp. 2073–2082, Apr. 2019.
- [15] H.-S. Ahn, Y. Chen, and H. Dou, "State-periodic adaptive compensation of cogging and Coulomb friction in permanent-magnet linear motors," *IEEE Trans. Magn.*, vol. 41, no. 1, pp. 90–98, Jan. 2005.
- [16] S.-L. Chen and T.-H. Hsieh, "Repetitive control design and implementation for linear motor machine tool," *Int. J. Mach. Tools Manuf.*, vol. 47, nos. 12–13, pp. 1807–1816, Oct. 2007.
- [17] Y. Li and Q. Xu, "Design and robust repetitive control of a new parallel-kinematic XY piezostage for Micro/Nanomanipulation," *IEEE/ASME Trans. Mechatronics*, vol. 17, no. 6, pp. 1120–1132, Dec. 2012.
- [18] T. H. Lee, K. K. Tan, S. Y. Lim, and H. F. Dou, "Iterative learning control of permanent magnet linear motor with relay automatic tuning," *Mechatronics*, vol. 10, nos. 1–2, pp. 169–190, Feb. 2000.
- [19] K. Kiong Tan, H. Dou, Y. Chen, and T. Heng Lee, "High precision linear motor control via relay-tuning and iterative learning based on zero-phase filtering," *IEEE Trans. Control Syst. Technol.*, vol. 9, no. 2, pp. 244–253, Mar. 2001.

- [20] K. Cho, J. Kim, S. B. Choi, and S. Oh, "A high-precision motion control based on a periodic adaptive disturbance observer in a PMLSM," *IEEE/ASME Trans. Mechatronics*, vol. 20, no. 5, pp. 2158–2171, Oct. 2015.
- [21] B. Yao and C. Jiang, "Advanced motion control: From classical PID to nonlinear adaptive robust control," in *Proc. 11th IEEE Int. Workshop Adv. Motion Control (AMC)*, Mar. 2010, pp. 815–829.
- [22] G. W. McLean, "Review of recent progress in linear motors," *IEE Proc. B, Electr. Power Appl.*, vol. 135, no. 6, pp. 380–416, Nov. 1988.
- [23] J. Yao, Z. Jiao, and D. Ma, "Adaptive robust control of DC motors with extended state observer," *IEEE Trans. Ind. Electron.*, vol. 61, no. 7, pp. 3630–3637, Jul. 2014.



KWANGHYUN CHO (Member, IEEE) received the B.S. degree in electrical engineering and computer science from Kyungpook National University, Daegu, South Korea, in 2008, and the M.S. and Ph.D. degrees in mechanical engineering from the Korea Advanced Institute of Science and Technology (KAIST), Daejeon, South Korea, in 2010 and 2014, respectively. He is currently a Senior Engineer with the Mechatronics Research and Development Center, Samsung Electronics

Company Ltd., Hwaseong-si, Gyeonggi-do, South Korea. His research interest includes precision motion control-based on linear motors.



KANGHYUN NAM (Member, IEEE) received the B.S. degree in mechanical engineering from Kyungpook National University, Daegu, South Korea, in 2007, the M.S. degree in mechanical engineering from the Korea Advanced Institute of Science and Technology, Daejeon, South Korea, in 2009, and the Ph.D. degree in electrical engineering from The University of Tokyo, Tokyo, Japan, in 2012.

From 2012 to 2015, he was a Senior Engineer with Samsung Electronics Company Ltd., Gyeonggi-do, South Korea. Since 2015, he has been an Assistant Professor with the School of Mechanical Engineering, Yeungnam University, Gyeongbuk, South Korea. His research interests include motion control, vehicle dynamics and control, and electric vehicles.

Dr. Nam is a member of the Korean Society of Automotive Engineers. He received the 2013 Best Paper Award from the IEEE Transaction on Industrial Electronics, in 2014.

...